Thermosensitive Nanostructures Comprising Gold Nanoparticles Grafted with Block Copolymers

ARTICLE *in* ADVANCED FUNCTIONAL MATERIALS · NOVEMBER 2007

Impact Factor: 11.81 · DOI: 10.1002/adfm.200700427

FULL PAPER

ADVANCED FUNCTIONAL MATERIALS

DOI: 10.1002/adfm.200700427

Thermosensitive Nanostructures Comprising Gold Nanoparticles Grafted with Block Copolymers**

By *Dongxiang Li*, *Yue Cui*, *Kewei Wang*, *Qiang He*, *Xuehai Yan*, and *Junbai Li**

Binary thermosensitive nanocomposites are fabricated by grafting block copolymers of poly(*N*-isopropylacrylamide) and poly(methoxy-oligo(ethylene glycol) methacrylate) onto gold nanoparticles through consecutive, surface-initiated, atom-transfer radical polymerization (ATRP). These Au@copolymer nanocomposites display a well-defined core/shell nanostructure and have two thermosensitive points near 33 and 55 °C in an aqueous suspension corresponding to the thermally induced conformational transition of inner homopolymer segments and outer oligo(ethylene glycol)-containing copolymer layer, respectively. Silver nanoparticles trapped within Au@copolymer nanocomposites with weakly crosslinked shells display thermally modulated catalytic activity as heterogeneous catalysts because of the thermosensitive collapse of the polymer layers.

1. Introduction

Recently, hybrid organic/inorganic nanocomposites have attracted increasing attention because of their potential in optics, magnetics, and electronics applications.[1] Many polymers have been employed to decorate gold nanoparticles in order to build new materials for different purposes.[2] Atom-transfer radical polymerization (ATRP) as a relatively new method displays several advantages in fabricating core/shell nanostructures, such as easy manipulation and the ability to control molecular weight, especially in modifying nanoparticles based on a "graft-from" strategy.[3] As an intensively studied thermosensitive polymer, poly(*N*-isopropylacrylamide) (PNIPAAM) undergoes a thermosensitive conformation change at a lower critical solution temperature (LCST) near 32 °C in aqueous solution.[4] Poly(methoxy-oligo(ethylene glycol) methacrylate) (PMOEGMA) has also been investigated as a thermosensitive water-soluble polymer, and its transformation temperature is related to the length of the oligo(ethylene glycol) moieties as well as the polymer molecular weight.[5] These environmentally stimuli-responsive polymers can be considered as intelligent materials with a variety of novel technological uses.[6]

Herein we report the fabrication of novel nanostructures of gold nanoparticles with a thermosensitive copolymer (Au@copolymer) by surface-initiated ATRP, as illustrated in Scheme 1. The initiator-modified gold nanoparticles (Au@initiator) are grafted with a block copolymer of PNIPAAM and PMOEGMA catalyzed by CuBr and *N*,*N*,*N*′,*N*′,*N*″-pentamethyldiethylenetriamine (PMDETA) in 2-propanol/water. Such an assembled core/shell nanostructure has a special response to temperature, exhibiting two critical points. Furthermore, silver nanoparticles embedded in these nanocomposites display thermally modulated catalytic activity as heterogeneous catalysts.

2. Results and Discussion

2.1. Preparation and Component Analysis

Surface-initiated ATRP, as shown in Scheme 1, was a consecutive "one-pot" multistage reaction at room temperature under a nitrogen atmosphere. In the first stage, the Au@initiator provided an excellent template for a living radical polymerization of *N*-isopropylacrylamide (NIPAAM) in a mixed 2-propanol/water solvent catalyzed by CuBr and PMDETA.[7] An appreciable amount of free initiator was added to the mixture to control the polymerization. Subsequently, methoxy-oligo(ethylene glycol) methacrylate (MOEGMA, number-average molecular weight, $M_n = 300$) monomer was added to the reaction system for the second copolymerization. The conversion of NIPAAM in the first homogeneous polymerization was about 1 % according to the chemometrical analysis, which includes the mass increase of modified gold nanoparticles and the obtained free polymer. The conversion of MOEGMA in the second stage was less than 1 %. Thus, because of the low monomer conversions, the second part of the copolymer could be considered as a random structure with unchanged components. PNIPAAM-

[*] Prof. J. B. Li, Dr. D. X. Li, Dr. Y. Cui, K. W. Wang, Dr. Q. He, X. H. Yan
Beijing National Laboratory for Molecular Sciences (BNLMS), International Joint Lab, CAS Key Lab of Colloid and Interface Science
Institute of Chemistry
Chinese Academy of Sciences
Beijing 100080 (P. R. China)
E-mail: jbli@iccas.ac.cn
Dr. Q. He
Max Planck Institute of Colloids and Interfaces
14476 Golm/Potsdam (Germany)

[**] This work is financially supported by NNSFC (Project Nos. 20574077, 20520130213, and 20471063), Chinese Academy of Sciences (kjcx2-sw-h12), and the collaborated project of the German Max-Planck Society. Supporting Information is available online from Wiley InterScience or from the author.

ADVANCED FUNCTIONAL MATERIALS

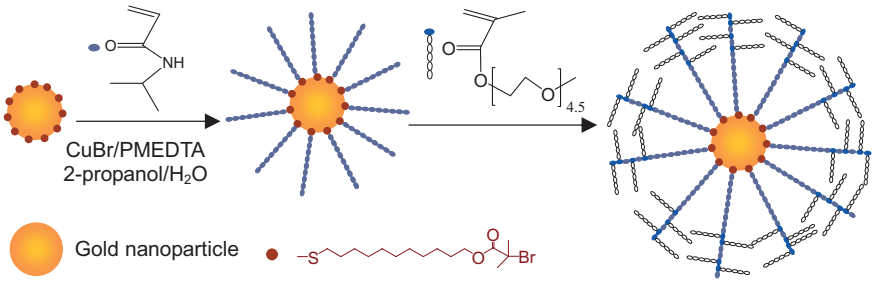

Scheme 1. Schematic showing the fabrication of Au@copolymer nanostructures.

grafted gold nanoparticles obtained in the first stage and the final Au@copolymer nanocomposites obtained after the second stage were separated by centrifugation and purified by washing, respectively. Their Fourier transform (FT) IR spectra are shown in Figure 1A. For PNIPAAM-grafted gold nanoparticles (curve a), the main characteristic peak assignments at 3297 cm^{-1} (secondary amide N–H stretch), 2971 cm^{-1} (CH_3 asymmetric stretch), 2928 and 2876 cm^{-1} (CH_2 stretches), and 1648 and 1544 cm^{-1} (secondary amide C=O stretches) are from the PNIPAAM segments.[7] For the Au@copolymer sample (curve b), new peaks at 1727 and 1104 cm^{-1} correspond to the characteristic carbonyl stretches of methacrylate and ether (C–O–C) bond stretches, respectively.[8] An X-ray photoelectron spectroscopy (XPS) survey profile of the Au@copolymer nanocomposite, shown in Figure 1B, confirms that the elemental components are C (74.3 %), O (20.4 %), N (5.22 %), Au (0.1 %), and a weak S signal. The deconvolution of the C 1s spectrum in Figure 1C shows five peak components with binding energies at 284.7, 285.6, 286.3, 287.5, and 288.4 eV,[9] which are attributed to different carbon atoms in the molecular structure, as shown in the inset of Figure 1C. All of these component analyses demonstrate that the designed Au@copolymer nanocomposites were successfully obtained from a consecutive ATRP reaction.

It is known that the molecular weight and molecular weight distribution of grafted polymers formed on surfaces are essentially identical to the values for free polymers formed from free initiator in surface-initiated ATRP.[10] The number average molecular weight of the free copolymer obtained by dialysis was approximately 45000 g mol^{-1} with a polydispersity of 1.99, as determined by gel permeation chromatography (GPC). The copolymer of PNIPAAM and PMOEGMA in the second copolymerization stage contained about 73 mol % PMOEGMA by the control experiment. According to quantitative analysis[11] of the ^1H NMR spectrum of the free copolymer, we determined that the inner PNIPAAM homopolymer has a molecular weight of 16 000 g mol^{-1}, and the outer PMOEGMA-containing copolymer layer has a molecular weight of about 29 000 g mol^{-1}.

2.2. Morphology and Structural Characterizations

Figure 2A and B show the transmission electron microscopy (TEM) images of Au@copolymer nanocomposites under different magnifications. The well-dispersed nanostructures consist of a gold "core" with an average diameter of 18 nm and a copolymer "shell" about 38 nm thick, which could be clearly observed after staining by phosphotungstic acid. Figure 2C displays a 3D atomic force microscopy (AFM) image of nanocomposites adsorbed on a newly cleaved mica surface. Each nanocomposite has a spherical center surrounded by a soft layer in an ordered array on the mica surface. The height of each central particle is about 20 nm, and the surrounding layer is approximately 1 nm according to the height section analysis. One particle surrounded by a soft layer (white circle shown in Fig. 2C) is approximately 205 nm in diameter. The separate particle in Figure 2D shows a "flowerlike" pattern, in which the center is mainly attributable to the gold core, while the "corona" is attributable to the comb-shaped polymer. The microscopy images directly confirm the designed structure of the Au@copolymer nanocomposites.

2.3. Thermosensitive Properties of Au@Copolymer Nanoparticles

It is well known that the thermosensitive PNIPAAM polymer has a very rapid swelling or shrinking response to temperature. Such a response involves a transformation from a hydrophilic to a hydrophobic state corresponding to the "intermolecular" and "intramolecular" hydrogen bonds below and above the LCST.[4] A previous study has demonstrated a dramatic red-shift of the surface plasmon resonance (SPR) of the suspension of PNIPAAM-grafted gold nanoparticles above 32 °C.[7b] Herein, we find that the Au@copolymer nanoparticles possess a similar property. Figure 3A shows the SPR peak of gold nanoparticles obtained from UV-vis spectra at different temperature. We found that the gold SPR peak always remained at 530 nm below 55 °C, but an obvious red-shift to 550 nm was observed above 55 °C (open circles). Simultaneously, the intensity of the spectral absorbance at 740 nm, I_{740}, exhibited a dramatic increase above 55 °C, as shown in Figure 3A (filled circles). In fact, such an SPR red-shift should not be caused by the thermosensitive property of PNIPAAM, as the transition temperature is far from its LCST. The thermosensitive response of Au@copolymer nanocomposites at 55 °C can only be ascribed to the thermosensitive change of the outer layer containing PMOEGMA chains. In order to prove this, we have performed a control experiment by copolymerizing NIPAAM and MOEGMA under the same conditions in an aqueous solution without gold particles. We found that the obtained copolymer had a phase-transition temperature at 55 °C (measurement results shown in Supporting Information, Fig. S1 and S2), similar to what was seen for Au@copolymer nanocomposites.

However, the SPR measurements did not provide any evidence for a thermally induced transformation of the PNIPAAM homopolymer, which is near 32 °C.[4] To determine

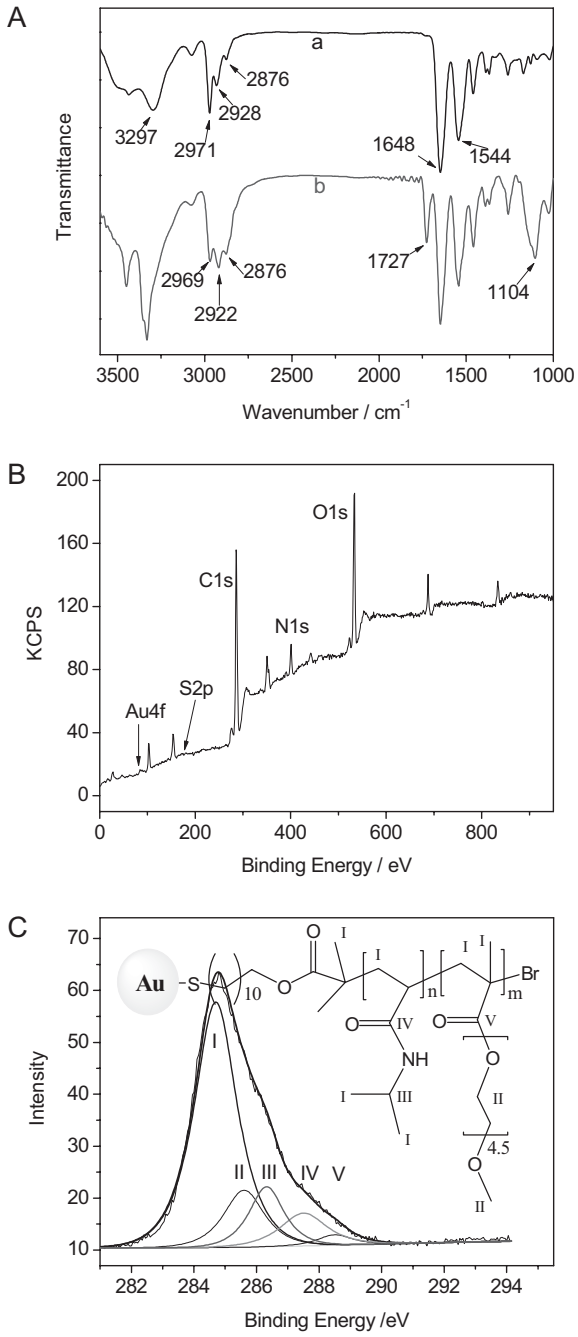

Figure 1. A) FTIR spectra of PNIPAAM-grafted gold nanoparticles (curve a) and the final Au@copolymer nanoparticles (curve b). B) XPS survey scan and C) the C 1s deconvolution of Au@copolymer nanoparticles on a CaF_2 plate.

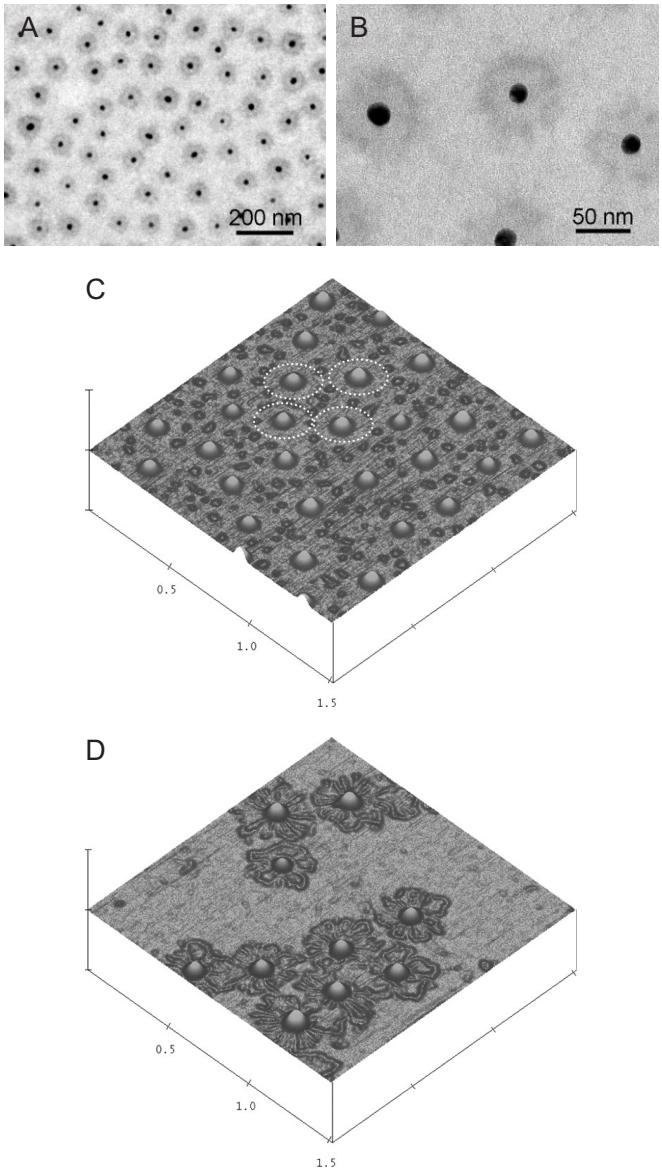

Figure 2. A,B) TEM and C,D) 3D AFM images of a Au@copolymer nanocomposite. AFM scale: 1.5 μm × 1.5 μm.

this transition, we subjected our materials to differential scanning calorimetry (DSC) analysis. Figure 3B shows the DSC curves of Au@copolymer nanocomposites obtained by heating and cooling the system. The baseline has a unilateral slope because of the solvent evaporation. We found that the thermosensitive point of the LCST of PNIPAAM appeared at 34.6 °C during heating and moved to 32.8 °C while cooling. In principle, the second transition of the copolymer should be detected by DSC as well. However, in our experiments, the DSC curves did not give an obvious signal at the second transition near 55 °C; we consider that this might be caused by a sample amount that was too small, as the measured liquid solution allowed a maximum volume of 20 μL, which led to a neglected contribution from PMOEGMA. But the second transition was clearly observed by SPR measurements. Thus we concluded from both DSC and SPR experiments that the Au@copolymer nanoparticles have two thermosensitive points near 33 °C and 55 °C, respectively, which are attributed to the contributions of the inner PNIPAAM homopolymer and the outer PMOEGMA-containing copolymer, respectively.

From the mechanism, we have learned that the polymer transformation from a water-soluble hydrophilic state to an insoluble hydrophobic state will eventually result in collapse of

ADVANCED FUNCTIONAL MATERIALS

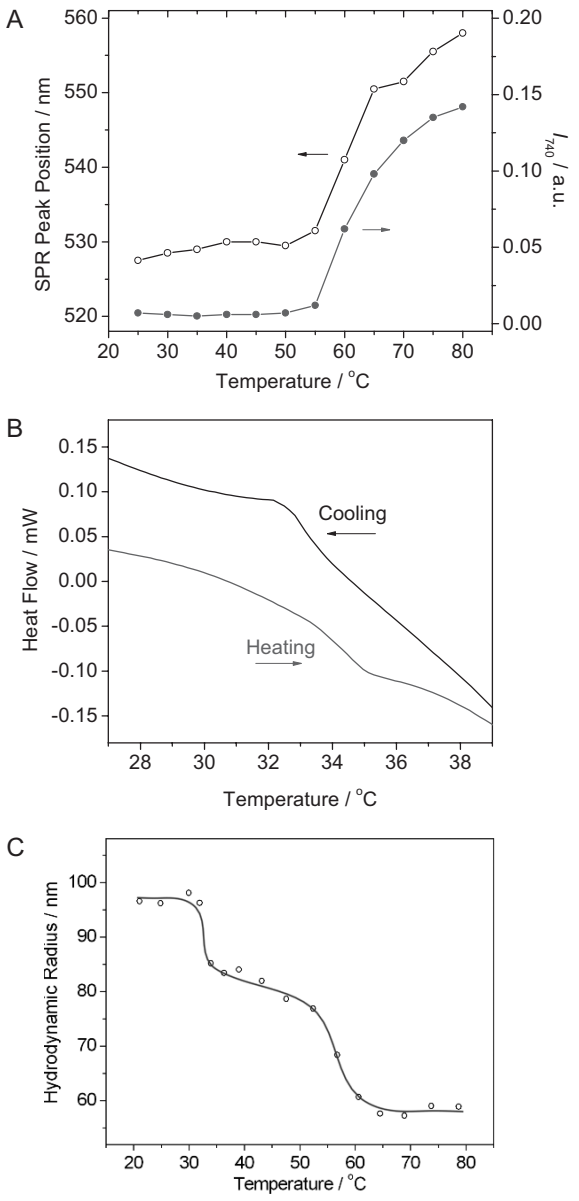

Figure 3. A) Profile of the SPR peak position, B) DSC curves, and C) hydrodynamic radius, R_h, of Au@copolymer nanoparticles in aqueous suspensions versus temperature.

the polymer chains. However, because the polymers are linked to the surface of the particles, the collapsed polymer should shrink onto the solid surface, which will cause the particle size to decrease. Dynamic light scattering (DLS) measurements verified that the Au@copolymer nanocomposite in aqueous suspensions had a two-step size decrease with increasing temperature, which is shown in Figure 3C and schematically illustrated in Scheme 2. As shown in Figure 3C, the measured hydrodynamic radius (R_h) of the Au@copolymer particles is about 96 nm at 25 °C. At this stage, the copolymer chains should be fully swelled.[4] When the temperature was above 33 °C, the inner PNIPAAM homopolymer became hydrophobic and collapsed onto the gold surface, causing a decrease in R_h to 82 nm at 40 °C. From the SPR measurements (Fig. 3A), we learned that no particle aggregation occurred at this temperature because of the protection of the outer copolymer layer. However, when the temperature was increased above 55 °C, PMOEGMA chains became hydrophobic and resulted in the second collapse of the copolymer chains,[5] which displayed a second decrease in R_h to 59 nm at 65 °C. We also found that the R_h at room temperature was similar to the size of the Au@copolymer nanocomposites obtained by AFM measurements, which was close to the actual particle size in aqueous suspension. In contrast, in a dried state the size estimated by TEM was obviously small.

2.4. Silver Nanoparticles Encapsulated in Au@Copolymer Nanocomposites

These thermosensitive Au@copolymer nanoparticles could be considered as carriers in the construction of environmentally responsive materials. Potential applications in biological system are anticipated, such as the delivery of biomolecules, drugs, and catalysts. It is known that a weakly crosslinked polymer network could enhance the ability for encapsulation. Hence, we used Au@copolymer nanocomposites with weakly crosslinked shells and explored their encapsulation ability.

The previous study of a PNIPAAM microgel demonstrated that a low crosslinking density could not significantly influence thermosensitive properties. For example, with 1 % crosslinker in the PNIPAAM copolymer, the LCST change was only less than 1 °C. [4e–g,7b] In our case, the FTIR spectra of Au@copolymer nanocomposites with weak crosslinking shells (See Supporting Information, Fig. S3) was similar to the spectrum of the sample that was not crosslinked, shown in Figure 1A (curve b). Thus the weakly crosslinked polymer shell of Au@copolymer nanocomposites could be assumed to have similar transition temperatures to the non-crosslinked shells. Figure 4A shows a typical TEM image of Au@copolymer nanoparticles with weakly crosslinked shells. A distinct margin was observed after the Au@copolymer nanoparticles were stained by phosphotungstic acid. The thickness of the polymer layers was estimated at about 25 nm, thinner than the non-crosslinked polymer shell. To explore potential applications of such Au@copolymer nanocomposites, silver ions were trapped in the polymer shell and were reduced in situ to silver nanoparticles by sodium borohydride. Then silver nanoparticles were immobilized in the crosslinked polymer shells to form embedded Ag nanoparticle nanocomposites. Figure 4B shows the UV-vis spectra of Au@copolymer nanocomposites and embedded Ag nanoparticle nanocomposites prepared under different concentration of silver ions. We observed peaks near 530 nm, which are attributed to the SPR of gold nanoparticles, and peaks near 390 nm, which are the contribution from silver nanoparticles. Moreover, the increase in silver ion concentration increased the ratio of the absorbance intensity from 390 to 530 nm. TEM images in Figure 4C and D display Ag nanoparticles embedded in the nanocomposites prepared at a low and high silver ion concentration, respectively. We estimated that about 15 silver nanoparticles approximately 1–3 nm in diameter were located

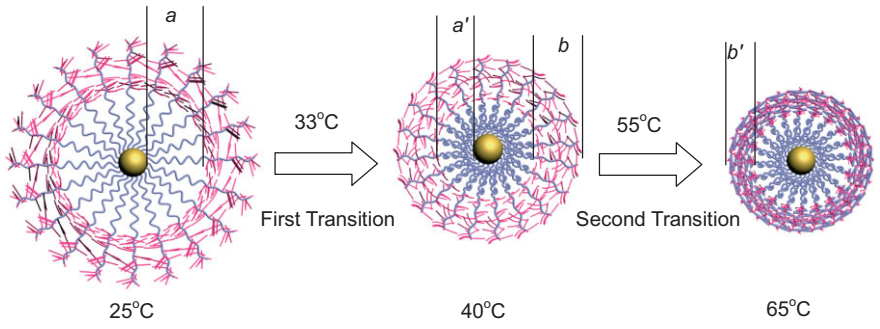

Scheme 2. Schematic illustrating the thermosensitive size change of Au@copolymer nanoparticles. The thickness of the inner layer, *a*, at 25 °C changes to *a′* at 40 °C above the first transition point, and the thickness of the outer layer, *b*, at 40 °C changes into *b′* at 65 °C above the second transition point.

Silver nanoparticles could heterogeneously catalyze the reduction reaction of 4-nitrophenol to aminophenol by sodium borohydride in aqueous suspensions, as reported previously.[12] The reduction kinetics could be easily monitored by UV-vis spectroscopy based on the quantitative relationship between the spectral absorbance at a wavelength of 400 nm and the concentration of the reactant 4-nitrophenate in high pH. In fact, gold nanoparticles could also catalyze the reduction reaction of 4-nitrophenol as reported elsewhere.[13] But in the present work, we demonstrated that the Au@copolymer nanocomposites did not possess catalytic activity because of the coating of the polymer layers on gold surface. Hence, we can use the Ag-nanoparticle-containing Au@copolymer nanocomposites to catalyze the above mentioned redox reaction. In the experiment, the concentration of sodium borohydride largely exceeded that of 4-nitrophenol; thus, first-order rate kinetics could be assumed with respect to the concentration, *c*, of 4-nitrophenate. Figure 5A shows the

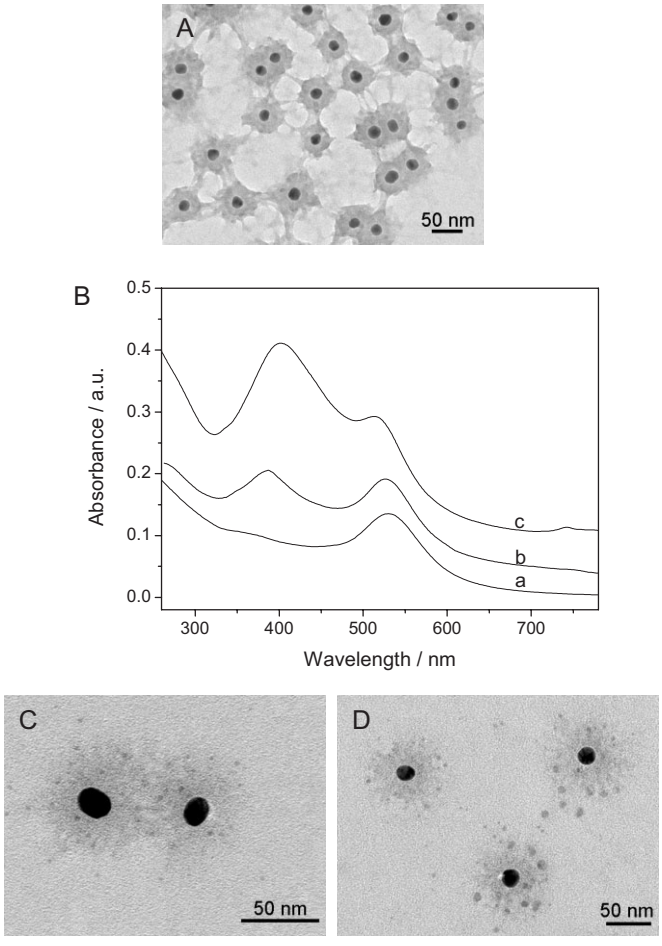

Figure 4. A,C,D) TEM images and B) UV-vis profiles of Au@copolymer nanocomposites with weakly crosslinked shells (curve a, image A) and a nanocomposite embedded with Ag nanoparticles prepared at low concentrations (curve b, image C) and high concentration of silver ions (curve c, image D).

in each Au@copolymer shells at low silver ion concentration (Fig. 4C), whereas more than 20 silver nanoparticles with a diameter in the range 2–8 nm were found in the Au@copolymer shells shown in Figure 4D.

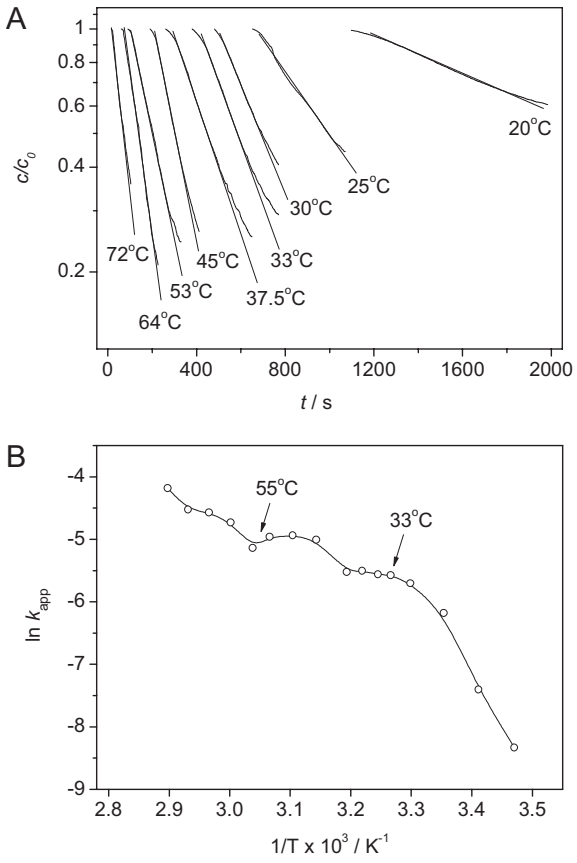

Figure 5. Kinetics of a 4-nitrophenol reduction catalyzed by a nanocomposite embedded with Ag nanoparticles. A) Linear fitting of $\ln[c/c_0]$ versus reaction time, *t*, from 15 to 72 °C. B) Arrhenius plot of the apparent rate constant, k_{app}, at different temperatures (*T*).

ADVANCED FUNCTIONAL MATERIALS

linear relationship between $\ln[c/c_0]$ and reaction time, t, at low conversions from 15 to 72 °C, where c_0 is the original concentration of 4-nitrophenol initially. It has been shown that the activation/introduction period of a Ag catalytic reaction strongly depends on the reaction temperature, which is consistent with that reported previously.[12,13]

According to kinetic mechanism, the apparent rate constant (k_{app}) can be calculated by linearly fitting $\ln[c/c_0]$ to t based on the first-order reaction assumption. Figure 5B gives the Arrhenius plot of k_{app} at different temperatures, T. It shows that a change in k_{app} values obviously deviates from the Arrhenius linear relationship between $\ln k_{app}$ and T^{-1}. In the heterogeneous catalytic system, k_{app} is usually proportional to the contact surface area (S) of silver nanoparticles;[12] thus the change in S will influence k_{app} values. In fact, the shrinking of the thermally induced polymer chains will reduce S for the catalysts.[12] As shown in Figure 5B, two critical transitions of k_{app} values appear near 33 and 55 °C, indicating that the catalytic activity of silver nanoparticles changes at these two points, which correspond to the thermosensitive transitions of the inner PNIPAAM homopolymer and the outer PMOEGMA-containing copolymer layer. Thus, we can deduce that silver nanoparticles embedded in such Au@copolymer shells have the capability to adjust their catalytic activity according to a temperature change. This property is particularly important for a system of silver nanoparticles involved as catalysts to control their reaction rate at rather high temperatures.

3. Conclusions

We fabricated a Au@copolymer nanocomposite with gold nanoparticles and a block copolymer of PNIPAAM and PMOEGMA via a consecutive "one-pot" multistage surface-initiated ATRP. The obtained nanocomposite had an obvious core/shell structure and possessed two thermosensitive points near 33 and 55 °C, which are attributed to the contributions of the inner layer, PNIPAAM homopolymer and the outer layer, PMOEGMA-containing copolymer, respectively. Such assembled Au@copolymer nanocomposites were able to trap silver nanoparticles. With the thermal response property of the coated copolymer, the embedded silver nanoparticles can modify their catalytic activity for controlling reaction rates.

4. Experimental

Materials: NIPAAM, MOEGMA ($M_n = 300$), and PMDETA were purchased from Aldrich. *N,N′*-methylenebisacrylamide (MBAA), CuBr, $HAuCl_4$, and other chemicals were obtained from Beijing Chemical Reagent Corp., China. The monomer NIPAAM was recrystallized from hexane, and MOEGMA was passed through an activated basic alumina column to remove the inhibitor. The deionized water was prepared in a three-stage Millipore Milli-Q Plus 185 purification system with a resistivity above 18.2 MΩ cm. All glassware was treated with a potassium dichromate/sulfuric acid digestant and then rinsed with tap water and deionized water.

The disulfide initiator $[S–(CH_2)_{11}–OCOC(CH_3)_2Br]_2$ was synthesized in our laboratory and characterized by ^1H and ^{13}C NMR spectroscopy and elemental analysis [14]. The initiator-modified gold nanoparticles (Au@initiator) were prepared from citrate-stabilized gold nanoparticles through a ligand exchange between the disulfide initiator and citrates in tetrahydrofuran (THF).

Fabrication of Au@Copolymer by ATRP: The target nanocomposite was fabricated with gold nanoparticles and a block copolymer of PNIPAAM and PMOEGMA (Au@copolymer) by surface-initiated ATRP. Typically, to a round-bottom flask was added NIPAAM (0.91 g), Au@initiator (2.0 mg), and CuBr (28.6 mg), and the mixture was degassed by three freeze-pump-thaw cycles under N_2. A degassed mixture of PMDETA (0.105 mL) and free initiator (2.0 mg) dissolved in 1.0 mL 2-propanol and 1.0 mL water was injected into the flask with vigorous stirring. After one hour growth of the PNIPAAM homopolymer, degassed MOEGMA (3.0 mL) was injected to the mixture, and the reaction was continuously performed for another hour. The system was opened to air for 20 min to terminate the reaction. Finally, the Au@copolymer nanocomposites were separated through centrifugation and were washed with 2-propanol and water. The separated supernatant was dialyzed in water to remove monomers and catalysts for component and molecular-weight analysis. The weakly crosslinked Au@copolymer samples were prepared by adding the crosslinker MBAA in a 1 mol % ratio to the monomers in the polymerization.

Control Experiment for Copolymer Component Determination: The recipe above was doubled for the control experiment. To a round-bottom flask was added NIPAAM (1.81 g) and CuBr (57.2 mg) and was degassed by three freeze-pump-thaw cycles under N_2. A degassed mixture of PMDETA (0.420 mL), MOEGMA (6.0 mL), and the free initiator (4.8 mg) dissolved in 2-propanol (2.0 mL) and water (2.0 mL) was injected into the flask with vigorous stirring. The molar ratio of the two monomers, NIPAAM/MOEGMA, was about 1:1.3, which was identical to the ratio used for the fabrication of Au@copolymer particles. A certain volume of reaction mixture was carefully extracted after different reaction times and was dialyzed to purify the copolymers in semipermeable bags. The obtained samples were characterized by FTIR and ^1H NMR spectroscopy. The results indicated that the copolymer components of all samples were essentially the same after different reaction times, and contained approximately 73 mol % POMEGMA, as determined by quantitative calculations of ^1H NMR spectra.

Embedding Silver Nanoparticles: Au@copolymer nanocomposites with weakly crosslinked shells were employed to trap silver ions, which were chemical reduced in situ to silver nanoparticles by sodium borohydride. First, a small amount of silver nitrate (0.05–0.5 mg) was mixed with 2.0 mL of an aqueous Au@copolymer suspension, and the mixture was incubated for more than 3 h under shaking, followed by centrifuging to discard the non-adsorbed silver ions in the supernatant. Next the precipitate was redispersed in 2.0 mL water and mixed with sodium borohydride (1.0 mg in 0.5 mL H_2O) under gentle shaking, and silver nanoparticles embedded in nanocomposites were obtained.

Catalytic Experiments of Silver Nanoparticles: The catalytic activity measurements of the silver nanoparticles embedded in the nanocomposites were based on a catalytic reduction of nitrophenol to aminophenol. In detail, 0.85 mL of 0.2 mM 4-nitrophenol (pH 10) and 0.05 mL of the obtained suspension of the silver nanocomposite was added to a quartz cell as a substrate and incubated at a certain temperature in a water bath. UV-vis spectroscopy was also conducted at this same temperature. Then, 0.10 mL of a 10 mM sodium borohydride was added to the mixture, and the system absorbance at 400 nm was immediately recorded for 30 min. The apparent rate constant k_{app} was deduced by the data analysis.

Characterization and Instrumentations: FTIR and UV-vis spectra were recorded on a TENSOR 27 instrument (BRUCKER, Germany) and a U-3010 spectrometer (HITACHI, Japan), respectively. XPS analysis was performed on an ESCALab220i-XL electron spectrometer (VG Scientific) using a 300 W Al Kα radiation at about 3×10^{-9} mbar, and the binding energies were referenced to the C 1s line at 284.8 eV from adventitious carbon.

The morphology of Au@copolymer nanoparticles was obtained by TEM (JEM-2010, JOEL) and AFM (NanoScope IIIa, Veeco). DSC analysis was performed on a DSC-822e instrument (METTLER TOLEDO). DLS measurements were carried out from 20 to 80 °C on a

commercial spectrometer (ALV/DLS/SLS-5022F) equipped with a multi-τ digital time correlator (ALV5000), and a cylindrical 22 mW UNIPHASE He–Ne laser ($\lambda = 632.8$ nm) was used. A very dilute suspension of Au@copolymer nanoparticles was used in DLS measurements, and the apparent equivalent hydrodynamic radius (R_h) was obtained through data analysis using ALV5000 software.

Received: April 16, 2007
Revised: June 19, 2007
Published online: September 20, 2007

[1] a) R. B. Thompson, V. V. Ginzburg, M. W. Matsen, A. C. Balazs, *Science* **2001**, *292*, 2469. b) M. Hui, H. Chen, C. Shen, L. Hong, B. Huang, K. Chen, L. Chen, *Nature Mater.* **2006**, *5*, 102. c) J. Lee, A. O. Govorov, N. A. Kotov, *Angew. Chem. Int. Ed.* **2005**, *44*, 7439. d) H. Y. Zhao, X. L. Kang, L. Liu, *Macromolecules* **2005**, *38*, 10 619. e) V. R. R. Kumar, T. Pradeep, *J. Mater. Chem.* **2006**, *16*, 837. f) B. F. Pan, F. Gao, L. M. Ao, H. Y. Tian, R. He, D. X. Cui, *Colloids Surf. A* **2005**, *259*, 89.

[2] a) W. P. Wuelfing, S. M. Gross, D. T. Miles, R. W. Murray, *J. Am. Chem. Soc.* **1998**, *120*, 12 696. b) A. B. Lowe, B. S. Sumerlin, M. S. Donovan, C. L. McCormick, *J. Am. Chem. Soc.* **2002**, *124*, 11 562. c) T. Teranishi, I. Kiyokawa, M. Miyake, *Adv. Mater.* **1998**, *10*, 596. d) Y. Zhou, H. Itoh, T. Uemura, K. Naka, Y. Chujo, *Chem. Commun.* **2001**, 613.

[3] a) T. K. Mandal, M. S. Fleming, D. R. Walt, *Nano Lett.* **2002**, *2*, 3. b) K. Ohno, K. Koh, Y. Tsuji, T. Fukuda, *Macromolecules* **2002**, *35*, 8989. c) H. Duan, M. Kuang, D. Wang, D. G. Kurth, H. Möhwald, *Angew. Chem. Int. Ed.* **2005**, *44*, 1717. d) D. X. Li, Q. He, Y. Cui, J. B. Li, *Chem. Mater.* **2007**, *19*, 412.

[4] a) H. G. Schild, D. A. Tirrell, *J. Phys. Chem.* **1990**, *94*, 4352. b) E. C. Cho, J. Lee, K. Cho, *Macromolecules* **2003**, *36*, 9929. c) Z. Hu, X. Xia, *Adv. Mater.* **2004**, *16*, 305. d) T. Hellweg, C. D. Dewhurst, W. Eimer, K. Kratz, *Langmuir* **2004**, *20*, 4330. e) N. C. Woodward, B. Z. Chowdhry, M. J. Snowden, S. A. Leharne, P. C. Griffiths, A. L. Winnington, *Langmuir* **2003**, *19*, 3202. f) H. Inomata, K. Nagahama, S. Saito, *Macromolecules* **1994**, *27*, 6459. g) T. Hino, J. M. Prausnitz, *Polymer* **1998**, *39*, 3279. h) R. Pelton, *Adv. Colloid Interface Sci.* **2000**, *85*, 1.

[5] a) S. Han, M. Hagiwara, T. Ishizone, *Macromolecules* **2003**, *36*, 8312. b) D. J. Li, G. L. Jones, J. R. Dunlap, F. J. Hua, B. Zhao, *Langmuir* **2006**, *22*, 3344. c) M. M. Ali, H. D. H. Stover, *Macromolecules* **2004**, *37*, 5219. d) H. W. Ma, J. H. Hyun, P. Stiller, A. Chilkoti, *Adv. Mater.* **2004**, *16*, 338. e) H. Lee, E. Lee, D. K. Kim, N. K. Jang, Y. Y. Jeong, S. Jon, *J. Am. Chem. Soc.* **2006**, *128*, 7383.

[6] a) D. E. Bergbreiter, B. L. Case, Y. S. Liu, J. W. Caraway, *Macromolecules* **1998**, *31*, 6053. b) J. H. Kim, T. R. Lee, *Chem. Mater.* **2004**, *16*, 3647. c) C. Li, N. Gunari, K. Fischer, A. Janshoff, M. Schmidt, *Angew. Chem. Int. Ed.* **2004**, *43*, 1101.

[7] a) Y. Cui, C. Tao, S. P. Zheng, Q. He, S. F. Ai, J. B. Li, *Macromol. Chem. Rapid Commun.* **2005**, *26*, 1552. b) D. X. Li, Q. He, Y. Cui, K. W. Wang, X. M. Zhang, J. B. Li, *Chem. Eur. J.* **2007**, *13*, 2224. c) Q. He, A. Küller, M. Grunze, J. B. Li, *Langmuir* **2007**, *23*, 3981.

[8] Y. Huang, J. Wang, X.-B. Liu, H.-L. Zhang, X.-F. Chen, W.-C. Zhuang, X. Chen, C. Ye, X.-H. Wan, E.-Q. Chen, Q.-F. Zhou, *Polymer* **2005**, *46*, 10 148.

[9] F.-J. Xu, E.-T. Kang, K.-G. Neoh, *Biomaterials* **2006**, *27*, 2787.

[10] a) D. J. Li, X. Sheng, B. Zhao, *J. Am. Chem. Soc.* **2005**, *127*, 6248. b) K. Ohno, T. Morinaga, K. Koh, Y. Tsujii, T. Fukuda, *Macromolecules* **2005**, *38*, 2137. c) M. Save, G. Granvorka, J. Bernard, B. Charleux, C. Boissière, D. Grosso, C. Sanchez, *Macromol. Chem. Rapid Commun.* **2006**, *27*, 393. d) M. Ejaz, Y. Tsujii, T. Fukuda, *Polymer* **2001**, *42*, 6811.

[11] a) L. Tao, G. Mantovani, F. Lecolley, D. M. Haddleton, *J. Am. Chem. Soc.* **2004**, *126*, 13 220. b) Y. Z. You, C. Y. Hong, W. P. Wang, W. Q. Lu, C. Y. Pan, *Macromolecules* **2004**, *37*, 9761.

[12] a) N. Pradhan, A. Pal, T. Pal, *Colloids Surf. A* **2002**, *196*, 247. b) Y. Lu, Y. Mei, M. Drechsler, M. Ballauf, *Angew. Chem. Int. Ed.* **2006**, *45*, 813. c) K. Esumi. R. Isono, T. Yoshimura, *Langmuir* **2004**, *20*, 237.

[13] S. Panigrahi, S. Basu, S. Praharaj, S. Pande, S. Jana, A. Pal, S. K. Ghosh, T. Pal, *J. Phys. Chem. C* **2007**, *111*, 4596.

[14] R. R. Shah, D. Merreceyes, M. Husemann, I. Rees, N. L. Abbott, C. J. Hawker, J. L. Hedrick, *Macromolecules* **2000**, *33*, 597.